NMRF/RR/12/2017

RESEARCH REPORT

Study of a Thunderstorm event over North East India using NCMRWF Regional Unified Model

M. Venkatarami Reddy, Saji Mohandas, A. Jayakumar and E. N. Rajagopal

December 2017

National Centre for Medium Range Weather Forecasting
Ministry of Earth Sciences, Government of India
A-50, Sector-62, Noida-201 309, INDIA

Study of a Thunderstorm Event over North East India using NCMRWF Regional Unified Model

M. Venkatarami Reddy, Saji Mohandas,
A. Jayakumar and E. N. Rajagopal

National Centre for Medium Range Weather Forecasting

Ministry of Earth Sciences

A-50, Sector 62, Noida-201309, INDIA

December 2017

Ministry of Earth Sciences
National Centre for Medium Range Weather Forecasting
Document Control Data Sheet

1	Name of the Institute	National Centre for Medium Range Weather Forecasting
2	Document Number	*NMRF/RR/12/2017*
3	Date of publication	
4	Title of the document	Study of a Thunderstorm Event over North East India using NCMRWF Regional Unified Model
5	Type of Document	Research Report
6	No. of pages & Figures	26 & 22
7	Number of References	14
8	Author (s)	M.Venkatarami Reddy, Saji Mohandas, A. Jayakumar and E. N. Rajagopal
9	Originating Unit	NCMRWF
10	Abstract	In the present study, an attempt is made to validate the performance of the National Centre for Medium Range Weather Forecasting (NCMRWF) Unified Model mesoscale version (NCUM-R) forecast for a thunderstorm event over Guwahati and to study the fidelity of the model in predicting the thunderstorm event. The mesoscale model is run with two horizontal resolutions at 1.5 km and 330 m around Guwahati region. A thunderstorm, occurred between 8-11 UTC on 12 June 2016 over Guwahati, is studied and the sensitivity of the model with regards to its cloud scheme is analysed. The best combinations of parameters were selected to further validate the model with respect to its potential for thunderstorm predictions and the temporal and spatial characteristics.
11	Security classification	Non-Secure
12	Distribution	Unrestricted Distribution

Contents

Abstract

In the present study, an attempt is made to validate the performance of the National Centre for Medium Range Weather Forecasting (NCMRWF) Unified Model mesoscale version (NCUM-R) for a thunderstorm event over Guwahati and to study the fidelity of the model in predicting the thunderstorm event. The mesoscale model is run with two horizontal resolutions at 1.5 km and 330 m around Guwahati region. A thunderstorm, occurred between 8-11 UTC on 12 June 2016 over Guwahati, is studied and the sensitivity of the model with regards to its cloud scheme is analysed. The best combinations of parameters were selected to further validate the model with respect to its potential for thunderstorm predictions and the temporal and spatial characteristics.

1. INTRODUCTION

Thunderstorms over north east India have immense societal impact by affecting the life and livelihood of a large population. This necessitates its accurate prediction using very high resolution mesoscale models and equally effective forecast verification techniques (Lilly, 1990). Thunderstorms are challenging problems with its wide range of scale interactions and the detailed mesoscale processes involved need to be well understood and analysed to enhance the predictive capability of the mesoscale models. In the recent period the global models have reached a stage to be able to forecast the synoptic to higher end of mesoscale events in the medium range with reasonable level of accuracy. And the focus is now on predicting higher resolution details of the events.

The convection permitting resolutions of NCMRWF Unified mesoscale model (NCUM-R) are used for the simulation and study of the spatio-temporal variations of extreme weather events. These grid point models having very high resolutions are under constant development with the aim of simulating physical processes accurately by avoiding the requirement for sub grid-scale parameterization. There are not enough observations available to validate the meso-details and the availability of automatic weather stations (AWS) or radar observations, if available over the location, are essential for conducting such studies, and thus constraining the sample size for statistically significant validation of the events. With the current status of the km scale resolution of NCUM-R, still the cloud and convective processes are not well resolved as many times these are of the scale of few hundred meters depending on the complexity and spatial variability of the underlying land surface. This necessitates new techniques to be invented and adopted for the verification and estimation of the thunderstorm forecasting potential of these high resolution models.

In the present work, an attempt is made to validate the performance NCUM-R for a thunderstorm event over Guwahati. A thunderstorm, occurred between 8-11 UTC on 12 June 2016 over Guwahati (IMD Reports), is studied and the sensitivity of the model with regards to its cloud scheme is analysed. NCUM-R is run with two horizontal resolutions of 1.5 km and 330 m around Guwahati region with initial and boundary conditions from the global NCUM runs of 17 km horizontal resolution. Temporal variations of dynamic and thermo-dynamic parameters are analyzed and compared with the observations. An experiment is also carried out to study the sensitivity of the forecast of the event with respect to its cloud parameterization. Different combinations of vertical profiles of cloud generation parameter are used in the model to find out the best in simulating the thunderstorm event anywhere in the small domain of the 330 m resolution model. Further the various thunderstorm indices

were computed to assess the favorable conditions for the formation of thunderstorm.

2. DATA AND METHODOLOGY

We utilized NCMRWF high-resolution regional Unified Model (NCUM-R, Jayakumar et al., 2017) set up over Guwahati domain over northeast India at horizontal resolutions of 1.5 km and 330 m. The model is based on Singapore cloud-resolving domain version of tropical science configuration. The initial and lateral boundary conditions are derived from the current operational 17 km grid-length NCUM global model (Rakhi *et al*., 2016) based on the Even Newer Dynamics for General atmospheric modeling of environment (END Game) dynamical core (Wood *et al*., 2014). The model time steps are 60 s for 1.5 km and 12 s for 330 m and it uses 80 vertical levels with model top at 38.5 km, with 14 model levels below 1 km. The model contains some parameterized physical processes, including mixed-phase microphysics (based on Wilson and Ballard, 1999), radiation (based on Edwards and Slingo 1996) and land-surface (Best *et al*., 2011) scheme. Moisture conservation is switched on in 1.5 km model. Orography is derived from the NASA Shuttle Radar Topographic Mission (SRTM) 90 meter digital elevation map and ISRO land use/land cover (Lu/Lc) is used in this study. Cloud scheme is based on the diagnostic scheme of Smith (1990), by including the modifications by Wilson et al., (2004) and diagnostic cloud fraction is based on Gregory (1999). Clouds are allowed to form in the grid box much before the average Relative Humidity reaches 100%. RHcrit is the parameter which determines the relative humidity ratio at which the cloud starts forming at a particular level. Fixed RHcrit vertical profile is used here and the diagnostic scheme features a more constrained relationship between the cloud variables, where the Liquid Water Content (LWC) and cloud fractions are diagnosed.

GPM satellite and IMD gauge rainfall datasets were used for verifying the rainfall apart from the station datasets of rain gauge as well as AWS stations. All the 7 AWS stations inside the Guwahati domain of 330 m (Fig. 1) are used for validating spatial and temporal distribution of high frequency rainfall forecast products of these convection-permitting models. The 330 m model domain orography is also shown in Fig.1 which depicts higher orography covering the southern part of the domain. The focus of the entire study is on the small domain over Guwahati where it is difficult to predict the location specific rainfall distribution in minute details. So the capability of the model in predicting any possibility of thunderstorm or deep convective build-up within in the defined small domain is examined. Thunderstorm indices were computed which describes the precursors and favorable factors for thunderstorm formations and the various characteristics of the event under the study. ERA

analysis and MERR2 reanalysis products are used to compare with the model forecasts. Several experimental runs with a nested structure for 1.5 km and 330 m models were carried out with a range of RHcrit parameters modified at all levels in accordance with the lowest level RHcrit values of 96%, 97%, 99% and 100% and also with the moisture conservation off and on to tune the model for the best physics for thunderstorm simulations.

The thermodynamic indices are computed using parameters like, Relative humidity, Temperature, Latent and sensible heat fluxes, Pressure, OLR, Vertical Velocity, specific humidity, potential vorticity, divergence and convergence. The indices and variables used in the study are Convective Inhibition (CIN), Totals Totals (TT), Perceptible Water (PW), K Index (KI), Lifted index (LI), and vertical velocity at 500 hpa (W). These indices and variables are selected based on previous studies on favourable conditions for any thunderstorm event (Vujovic *et al.*, 2015; Wilks, 2006; Haklander and Van Delden, 2003; Kunz, 2007; Tyagi, 2011), such as conditional instability, moisture buildup, rapid rise of warm air and a mechanism to cause lifting of surface air (warm/cold front, orography, etc.). The analysis is done in respect of the causes of initiation of thunderstorm. These can be local heating, advection of air masses, orographic blocking and lifting, frontal movements and strong currents of sufficient depth.

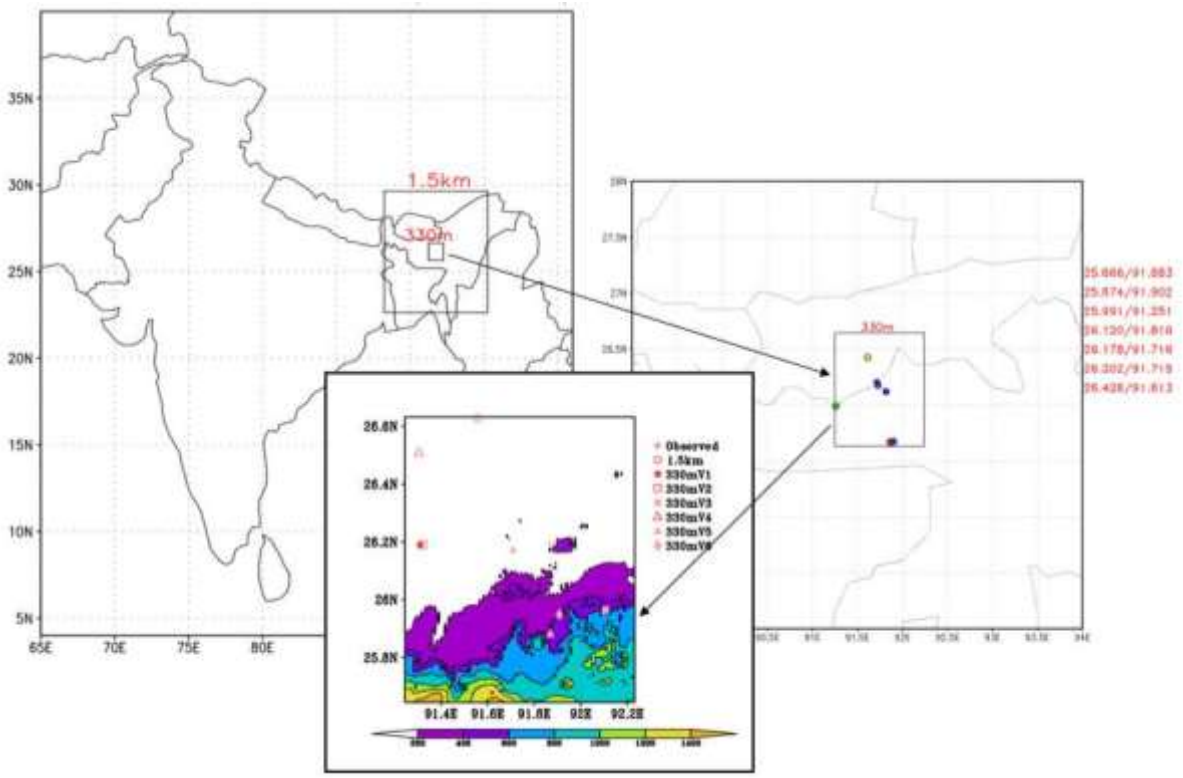

Fig. 1: *1.5 km and 330 m resolution model domains centred at Guwahati rain gauge station and the 7 AWS stations under the smallest domain (330 m model domain) for the thunderstorm study. Also shown the orography (shading) and the 3 hourly maximum rainfall (mm) locations in the experiments.*

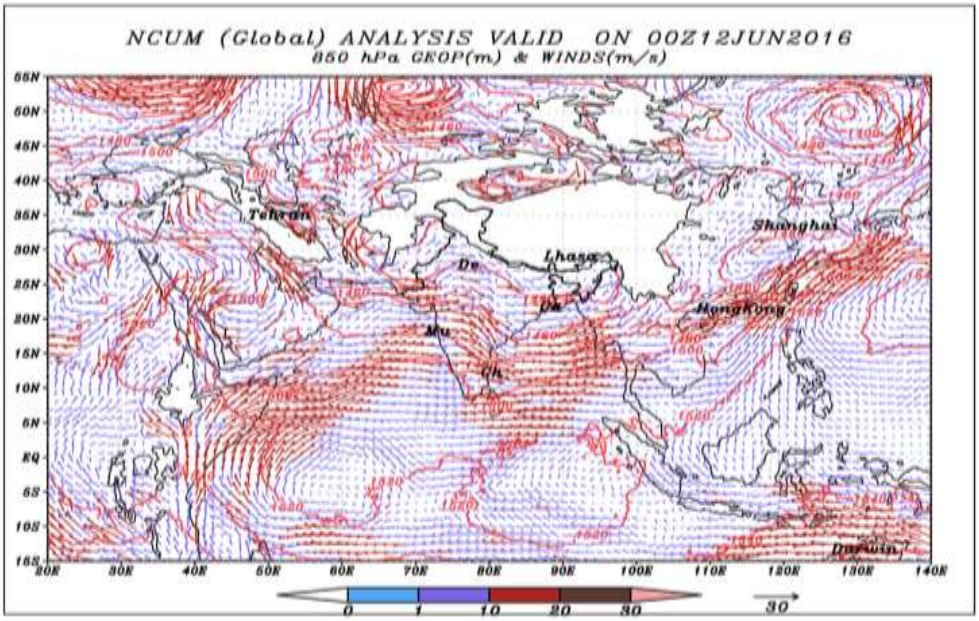

Fig. 2*: Wind (m/s) and geopotential (m) valid for 00 UTC, 12 June 2016 at 850 hPa in NCUM global model analysis.*

3. SYNOPTIC FEATURES AND ITS SIMULATION

The large-scale wind (m/s) and geopotential (m) pattern at 00 UTC 12 June 2016 at 850 hPa before the thunderstorm event from the NCUM global model analysis is shown in Fig. 2. From the figure, we can notice that the active monsoon conditions with strong cross equatorial flow and a north-south oriented trough over northeast India extending to North Bay of Bengal. Fig. 3 shows the down-scaled wind circulations for 1.5 km model at 925 hPa level for the same time. It indicates that the entire domain is dominated by strong incursion of south-westerly wind over the southwest corner of the domain. This south-westerly wind is diverted by the topography into mainly an anticyclone wind circulation around the terrain features, with the variations in wind speed and directions indicative of the irregular local terrain features. The strong south-westerly wind, which impinges on the orographic feature over the southern side of the 330 m model domain, splits and forces a cyclonic wind turning over the south of the inner box. A part of the low level winds turns anticyclone towards the north of the 330 m model domain encircling it within a predominating westerly flow. The high resolution orography in the convection-permitting models generates perturbations in the surface levels due to the detailed surface heterogeneity and the consequent secondary circulations. Thus the upper level trough induces localised circulations around the high terrain over the Guwahati region and leads to moisture convergence and confluence zones along with its eastward movement which causes the further build-up of deep cumulonimbus clouds over the region by the afternoon. This is shown in Fig. 4 (e-h), during the period of the thunderstorm, where the strong southerly wind is divided into a cyclonic and anti-cyclonic wings encircling the 330m model domain and converging over the northern part between 8 and 11 UTC the observed thunderstorm period, probably owing to the orographic undulations over the region. The mean sea level pressure (MSLP) pattern shows a decreasing trend especially over the northwest of 330 m model domain (Fig.4 (a-d)). Fig 5 shows the hourly outgoing long wave radiation (OLR) and rainfall distribution for the 1.5 km run during the thunderstorm period, where the thick deep clouds are seen to develop over the northwest part of the 330 m model domain, while the hourly rainfall is manifested as widely distributed and locally centred cellular structures that are mostly distributed over the valleys close to and north of 330 m model domain. The 330 m model is mostly devoid of any grid scale rain except over its northwest corner and parts of the valley over the Southside of the domain.

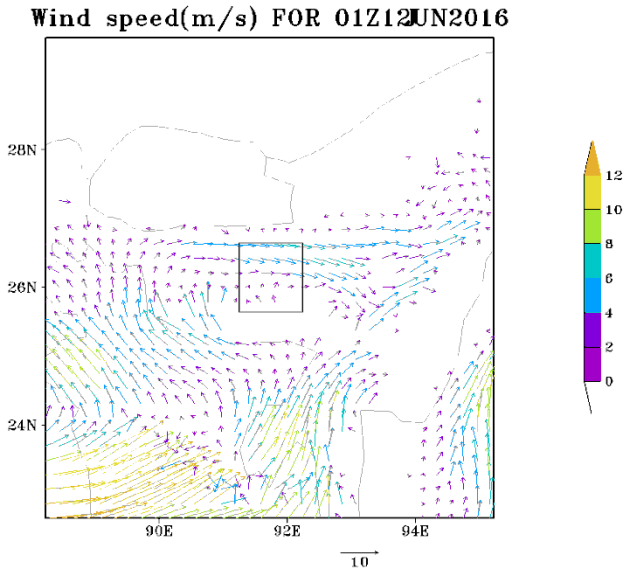

Fig. 3*: Wind distribution valid on 00 UTC, 12 June 2016 at 925 hPa in NCUM-R (1.5 km).*

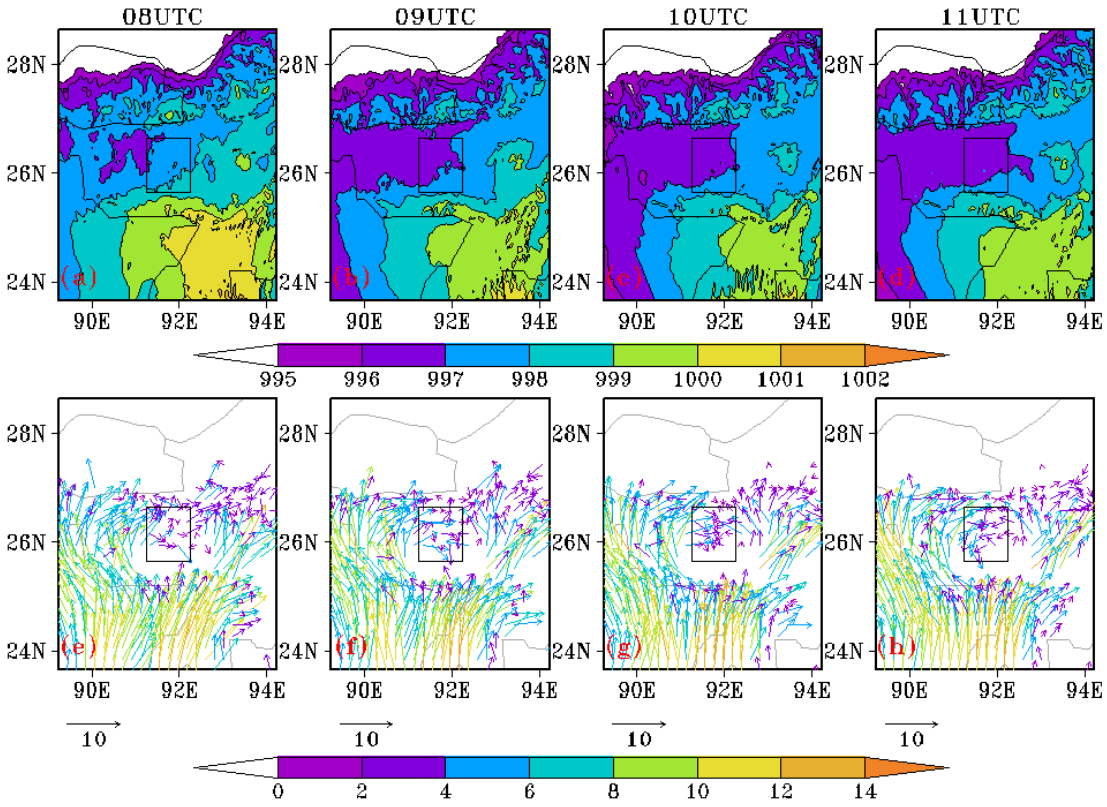

Fig. 4: *1.5 km NCUM model forecasts of hourly (08 UTC, 09 UTC, 10 UTC, and 11 UTC) spatial distribution of MSLP (hPa) (a-d) and Wind (m/s) distribution (e-h) at 925 hPa level for the thunderstorm on 12 June 2016.*

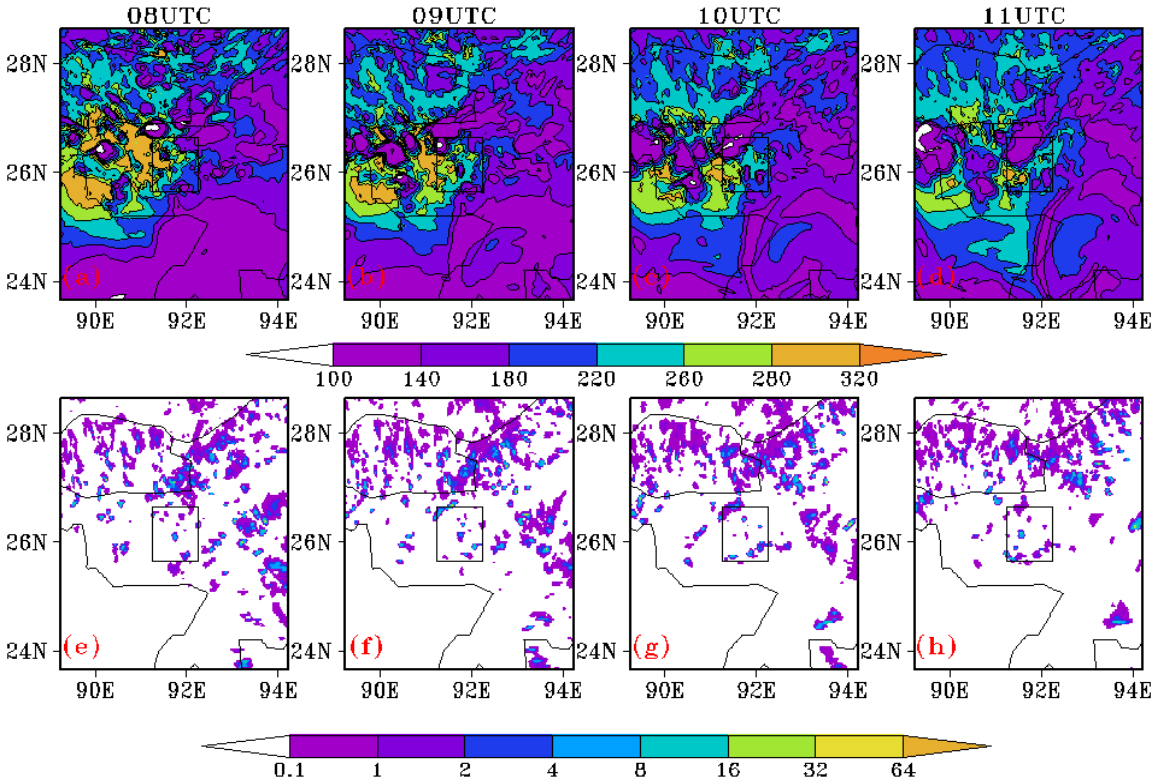

Fig. 5: *1.5 km NCUM-R model simulated hourly (08 UTC, 09 UTC, 10 UTC, and 11 UTC) spatial distribution of (a-d) OLR (Wm^{-2}) and (e-h) Rainfall (mm) for the thunderstorm on 12 June 2016.*

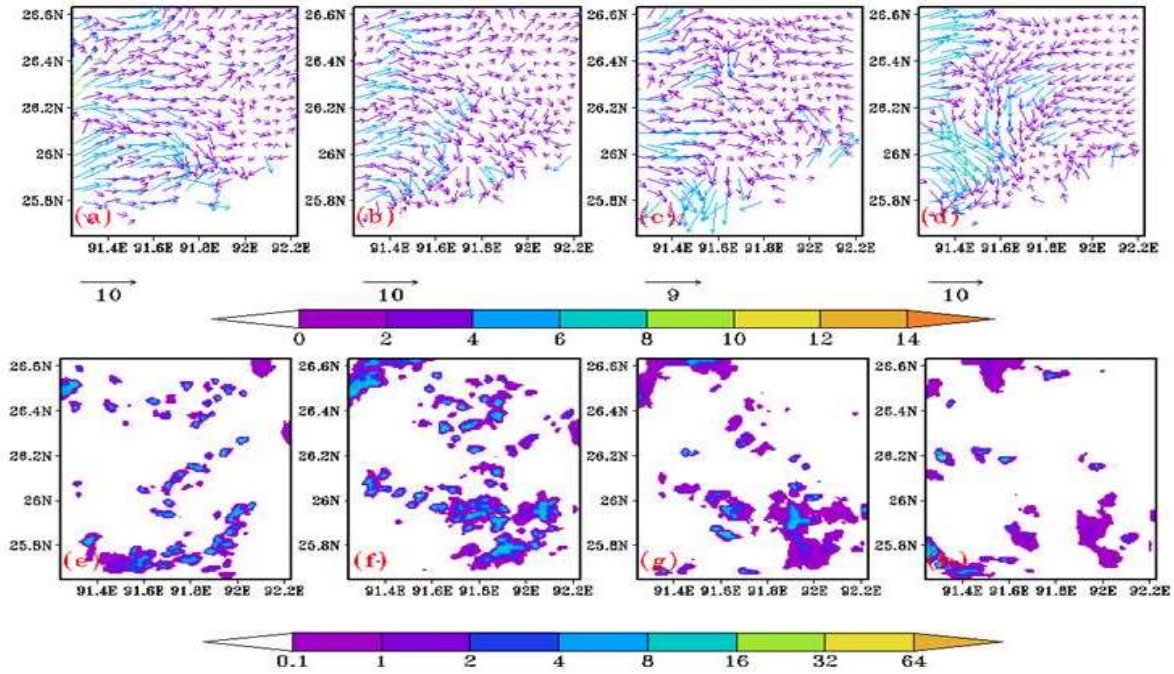

***Fig. 6**: 330 m NCUM-R simulated hourly (08 UTC, 09 UTC, 10 UTC, and 11 UTC) spatial distribution of (a-d) wind (m/s) at 925 hPa level and (e-h) rainfall (mm) for the thunderstorm on 12 June 2016.*

Though 330 m model forecasts show similar features more clearly, the wind pattern and rainfall distribution is verified (Fig. 6). The wind pattern is dominated by strong westerly flow over the western boundary of the domain impinging on the local hills to generate the transient circulation features and heavy localised cells of rainfall, ultimately forming a convergence line of strongly developed easterly and westerly making a north-south oriented shear line. The hourly rainfall cells are mostly located over the south and southeast sector of the domain, except for a heavy spell at 9 UTC over northwest corner. Fig. 7 shows the surface temperature and relative humidity distributions and transformations during the thunderstorm event. Figure shows the pockets of high temperatures over the northwest sector of the domain which are slowly decreasing due to the rainfall activity as the moist-laden cooler winds spreads westward with time. Similarly the humidity increases over the northwest sector and leads to cooling the entire domain with time during the thunderstorm events.

Fig. 8 shows the domain averaged parameters of zonal wind, meridional wind, vector wind speed and MSLP over the 330 m domain box for NCUM global (17 km), 1.5 km and 330 m resolutions on 12 June 2016. The global model values at 3 hourly intervals shows a large reversal in the direction of zonal wind from westerly to easterly before 9 UTC and continues even after 11 UTC, while the meridional component does not show much variability and remains with a weak southerly component, indicating the change in wind from west south westerlies to east south-easterlies. At around 18 UTC the wind turns to east north-easterly, with a slight temporary reduction in easterly component. Exactly at 9 UTC the wind speed shows the minimum value and MSLP also reduces to its lowest mark, indicating prerequisites of extreme weather conditions in the grid box area even at 17 km resolution.

Both 1.5 km and 330 m models show more or less similar features with much more temporal variability due to the better defined orography influencing the surface wind creating more flow drags and gustiness. There is a change from stronger westerly components towards weaker easterlies during the thunderstorm period, and remains weak for the rest of the day. However, the meridional component in the high resolution runs shows much more kinetic energy compared to the global model, channelling the flow from strong southerlies to northerlies during the thunderstorm event. The vector wind speed shows continuous reduction till late evening in contrast to the global run, while MSLP shows the similar wave-like trend as that of global model run though the high resolution runs shows more deep system compared to the global model.

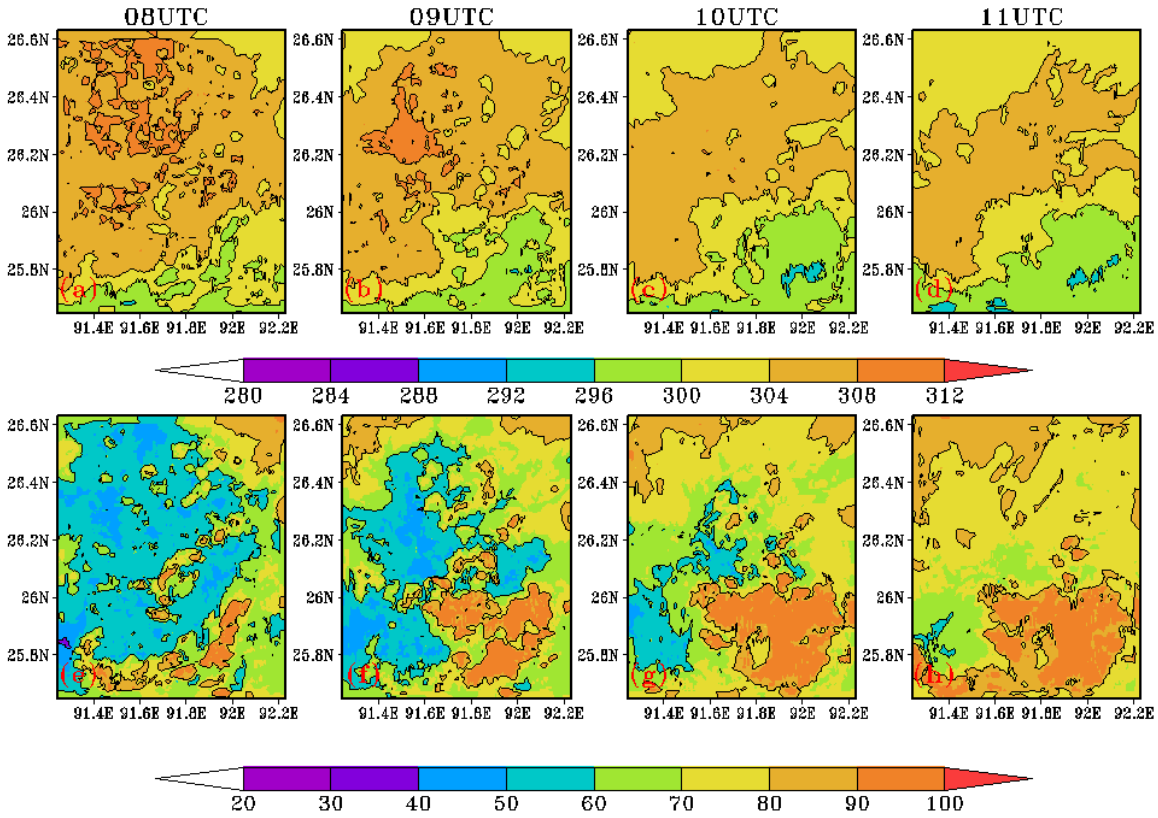

Fig. 7: *330 m model simulated hourly (08 UTC, 09 UTC, 10 UTC, and 11 UTC) spatial distribution of (a-d) Temperature (K) and (e-h) Relative Humidity (%) for the thunderstorm on 12 June 2016.*

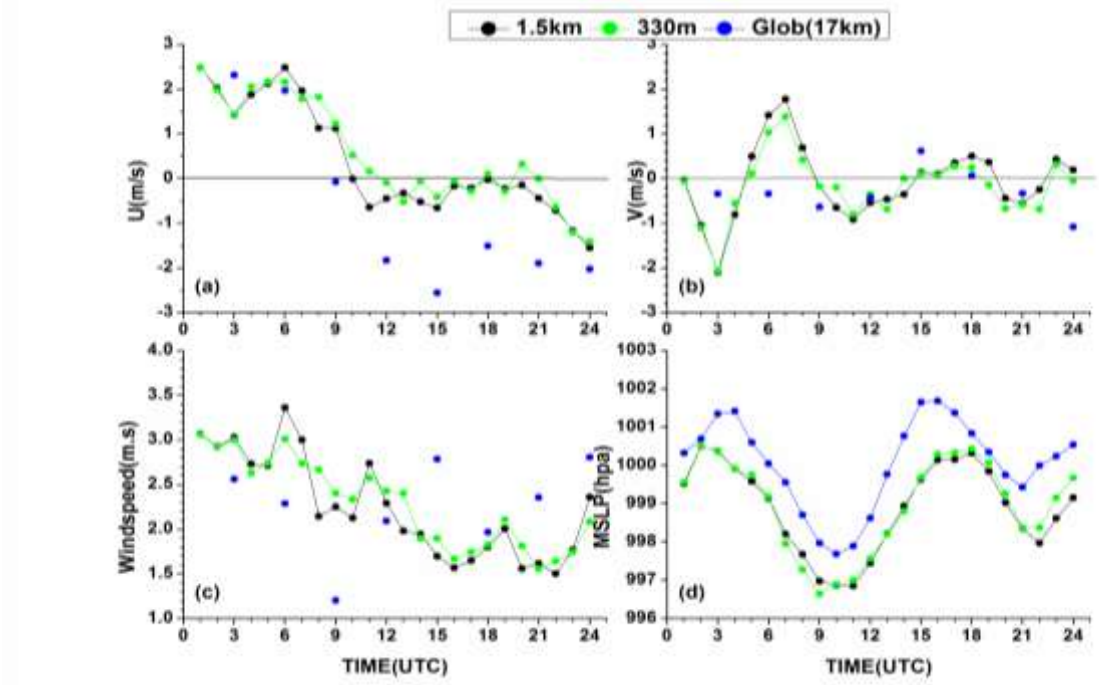

Fig .8 : *NCUM Global (17 km), regional (1.5 km and 330 m) predicted 330 m model average meteorological variables (a) Zonal Wind speed (U; m/s), (b) Meridional wind speed (V; m/s), (c) Wind speed (m/s) at 925 hPa level and (d) MSLP (hPa).*

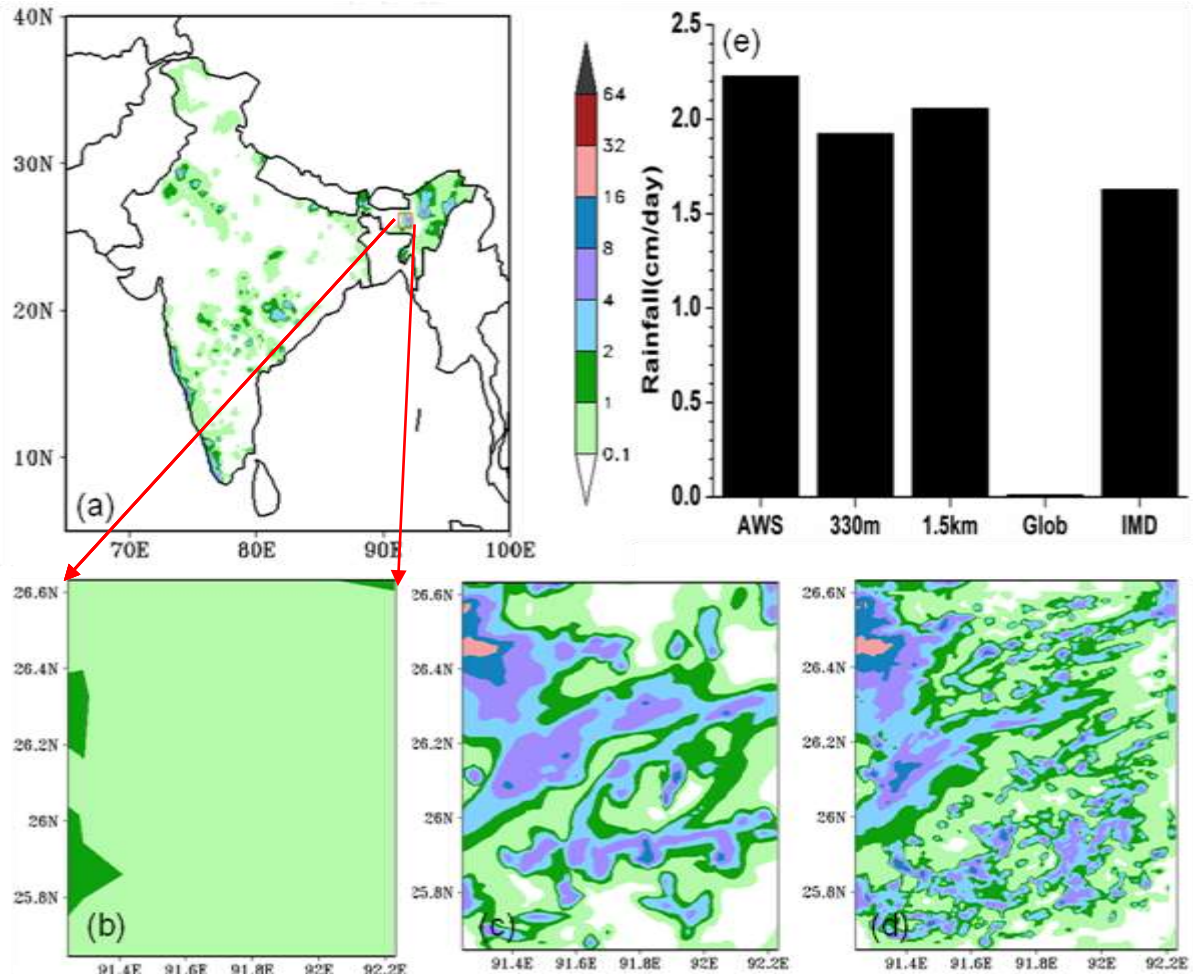

Fig. 9: *Observed and NCUM simulated rainfall (cm/day) for (a) IMD rain gauge, (b) global model (17 km), (c) regional model (1.5 km), (d) regional model (330 m) and (e) Comparison of daily rainfall averaged over (25.645°N-26.631°N, 91.245°E-92.231°E).*

Fig. 9 shows the mean accumulated daily rainfall of the thunderstorm day on June 12, 2016, obtained from IMD rain gauge stations data (Fig. 9a) and the model runs (Fig. 9b-d). On June 12, 2016 the selected grid region (represented with square box in Fig. 9a) has the rainfall amounts in the range of 4-8 cm/day, whereas the NCUM global model output with 17 km resolution showed a rainfall values ranging from 0.1-1 cm/day over the selected region. The rainfall amounts obtained with high resolution models range from 4 to 8 cm/day for the selected region, which are comparable with the observed rainfall. There are heavy rainfall contours more than 32 cm (red colour) over the northwest part in both 1.5 km and 330 m, while 330 m model shows more spatial variability. The domain averaged rainfall (Fig. 9e) clearly shows that the high resolution runs are able to produce comparable amounts of rainfall over the selected domain while global model is unable to resolve the heavy rainfall event. Also the domain averaged rainfall from 1.5 km run is more close to the observation than 330

m run though the difference between 1.5 km and 330 m rainfalls is not very significant. Hence the aim of this study is to test and tune the science settings to enhance the performance of the latter.

4. SIMULATED THUNDERSTORM CHARACHERISTICS

The simulated characteristics of the thunderstorm event by the high resolution models at 1.5 km and 330 m resolutions were analysed to see how well the large scale conditions and the feedbacks are simulated during the thunderstorm period. To validate the model, various meteorological parameters [Temperature, Outgoing Longwave Radiation (OLR), and surface latent heat (LH) flux] from MERRA2 hourly data available with $0.5^{\circ} \times 0.625^{\circ}$ resolution are used. The three hourly spatial variation of surface temperature from 06 to 15 UTC on June 12, 2016, obtained from MERRA2 and NCUM-R (1.5 km) are shown in Fig. 10 (a-d) and Fig. 10 (e-h) respectively. From Fig. 10 it is clear that build-up and subsequent reduction of surface temperature with the time (from 06 UTC to 15 UTC) can be seen clearly in both model and MERRA2 reanalysis. As the model resolution is very high compared to the observations, the model shows high resolution features and spatial variations. Apart from that, overall it can be concluded that both shows fairly good match with surface (1.5 m) temperatures decreasing over the thunderstorm domain soon after 9 UTC.

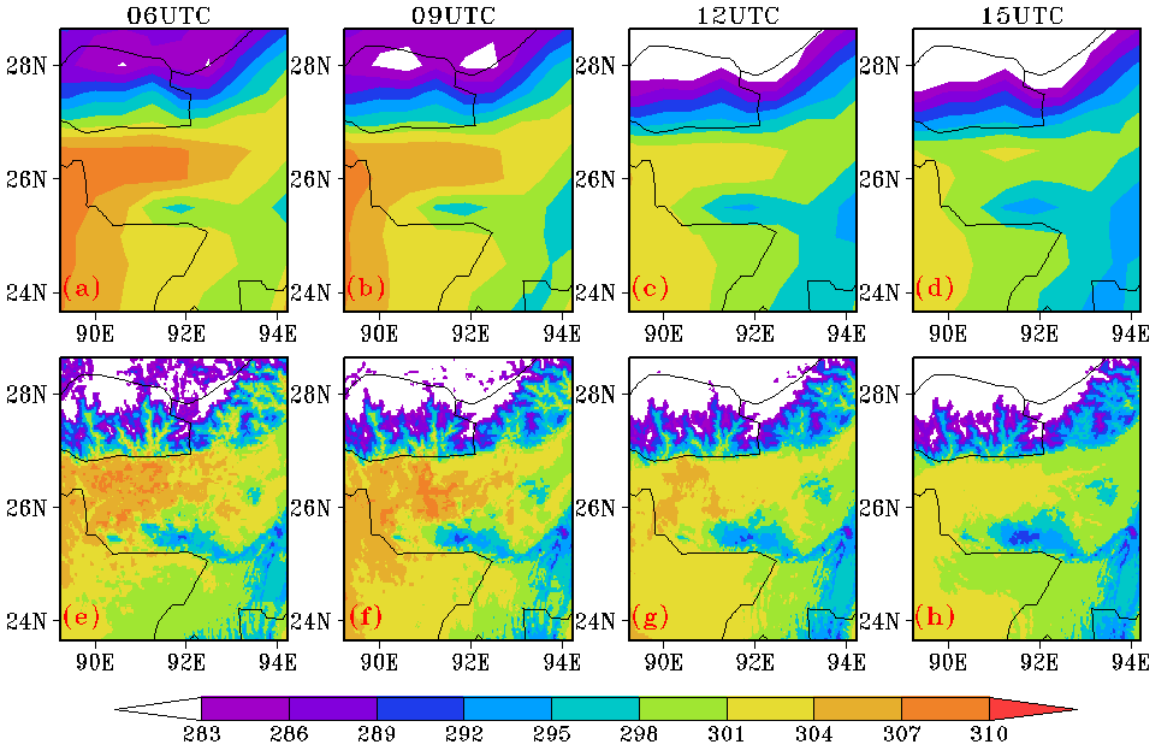

Fig. 10: *Observed and model simulated three hourly (06 UTC, 09 UTC, 12 UTC, and 15 UTC) spatial distribution of surface temperature (K) obtained with MERRA2 (a-d) and 1.5 km resolution NCUM model (e-h) for the thunderstorm on 12 June 2016.*

The three hourly spatial variation of outgoing long wave radiation (OLR) (Fig.11) shows that the OLR is relatively low during thunderstorms period (09 UTC) when compared to before (06 UTC) and after thunderstorm periods (12 UTC and 15 UTC). This may indicate the increase in deep clouds over the domain of our interest and there is a fairly good agreement with the reanalysis though the model shows more spatial variations. It can be seen that there is a patch of higher OLR values over the northwest corner of the 330 m model domain through-out the thunderstorm period and there is some eastward migration of the patch towards the centre of the domain during the period. 330 m model shows more intense patches and spatial variations due to the spatial undulations of the terrain.

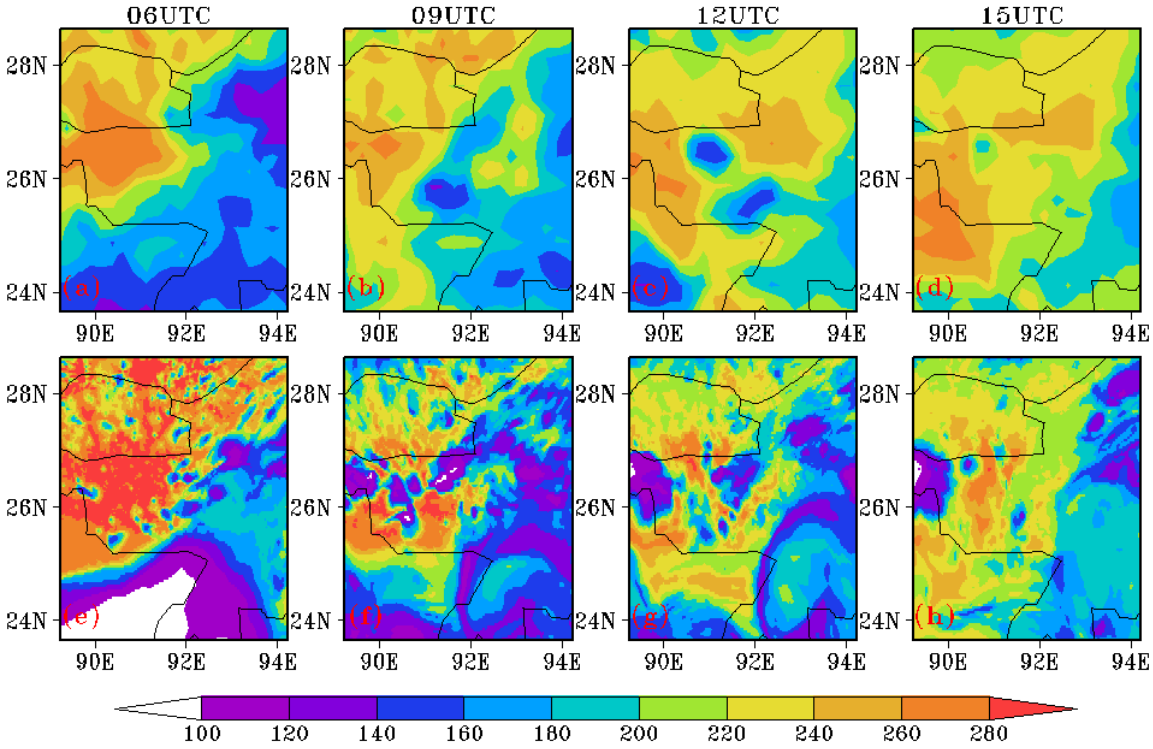

Fig. 11: *Same as* ***Fig. 10*** *except spatial distribution of OLR (W/m^2)*

The domain averaged (91.2^o -92.2^o E and 25.6^o N-26.6^o N) rainfall, relative humidity, outgoing long wave radiation (OLR), surface temperature, and convective available potential energy (CAPE) are shown in Figure 12(a), 12(b), 12(c), 12(d), and 12(e) respectively. These values are obtained from AWS (seven stations averaged values), 330 m and 1.5 km model resolution, and from other observational data set [Rainfall-GPM (0.1° × 0.1°), RH & Temp-Merra2 (0.5° × 0.625°), OLR- Kalpana-1 VHRR (0.25° × 0.25°)]. The mean rainfall amounts over the selected domain are observed in 1.5 km and 330 m resolutions models from 04 UTC to 24 UTC of June 12, 2016. The AWS recorded the rainfall over the domain from 06 UTC to 12 UTC and from 21-24 UTC. The time variation of relative humidity (RH) obtained from

1.5 km model resolution, 330 m resolution, and AWS are shown in Figure 12b. In both observations and model results, RH decreases from 00-07 UTC and then increases from 07-24 UTC. However the AWS observed RH decreased once again from 18-24 UTC. The models are able to predict the mean RH time variation, except that there is some time delay from the observation, which is also reflected in the peak domain mean rainfall timings. The time variation of OLR obtained from remote sensing (denoted as observed), and model values with 330 m and 1.5 km resolution are shown in Fig. 12e. In both 330 m and 1.5 km resolution models, OLR values are gradually decreased from 00-12 UTC. However, this decreasing trend of OLR is relatively high in the observations when compared to model OLR values, which is again well simulated by 4 km model domain mean OLR. The temporal evolution of surface temperature obtained from AWS, 330 m model resolution, 1.5 km model resolution and observations are shown in Figure 12d. In both observations (AWS and Satellite) the surface temperature increases up to 07 UTC and thereafter decreases. However, this decrease of surface temperature is not simulated by any of the models. In both 330m and 1.5 km resolution, the model results show clearly the increase in CAPE values from 07 UTC to ~17 UTC (Fig. 12e). However, this tendency to reduce the cloud cover soon after the event is absent in the observation and 4 km runs. The 4 km model domain averaged values are different from other model runs.

We analysed the various parameters in the 330 m model domain box at 1.5 km and 330 m resolutions for assessing the performance as how good is each of them in predicting any thunderstorm event or deep convective showers anywhere inside the small box. We compared time variation of the observations at Guwahati station location (26.17°N and 91.71°E) with the model parameters (Fig. 13). The observed rainfall started at 9 UTC peaking at 11 UTC with the peak rainfall value of around 15 mm. The 1.5 km model drastically under predicted the rainfall (Fig. 13a), which occurred at slightly an earlier time to that of the observed rainfall. Similarly 330 m model predicted only very trace amount of rainfall with more delay. So we compared each of the model runs at its maximum rainfall point in the box during the 3 hour period (8-11 UTC) for the observed parameters at the thunderstorm location of Guwahati, to see whether the models show deep convective activity anywhere in the box relatively at the similar time period of the actual occurrence. At the grid point of maximum rainfall inside the box (Fig. 14), both the 1.5 km and 330 m models over predicted the rainfall when compared to the observations, whereas the 330 m model results are closer to the observations. Here also the forecast rain is predicted slightly earlier than observed for both the models.

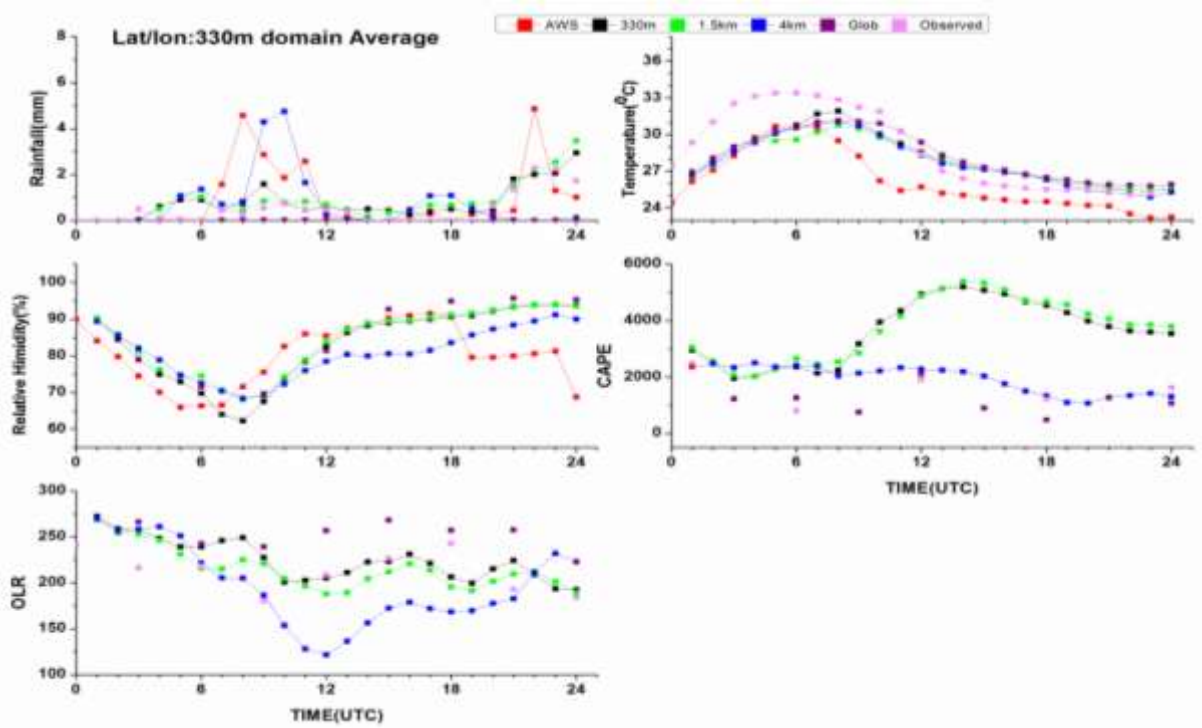

Fig. 12: *Temporal variations in domain averaged rainfall (mm), temperature (K), relative humidity (%), CAPE (J/kg), OLR (W/m^2) from NCUM Global (17 km), regional (4 km, 1.5 km and 330 m) models along with observations from available of Automated Weather Stations (AWS) station and satellite observations (Rainfall-GPM, RH & Temp-Merra2, OLR- kalpana-1 VHRR).*

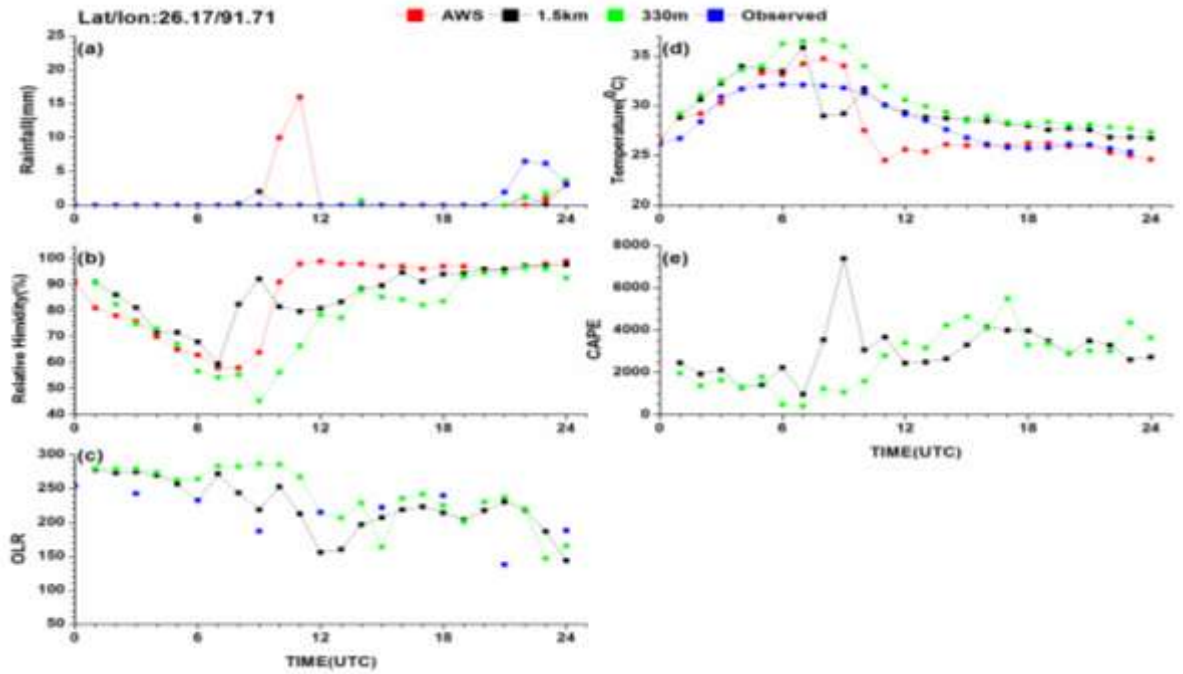

Fig. 13: *Temporal variation of meteorological variables from NCUM regional (1.5 km and 330 m) model, Automated Weather Stations (AWS) and observed (OLR- kalpana-1 VHRR) at 26.17°N/91.71°E.*

The other parameters like relative humidity (Fig. 14b), OLR (Fig.14c), temperature (Fig.14d), and CAPE (Fig.14e) are comparable both in observations and models; though in each model the timings are slightly out of phase. It is to be noted that there is a significant decrease in temperature during the period of thunderstorm in the observation whereas the models are predicting lesser rate of reduction in temperature after the event, which is observed from Fig. 13. A sudden increase in RH from 60% to 100 % occurred during the thunderstorm period i.e., from 08 UTC to 11 UTC in the observation. The models are also showing an increase in RH which is matching more or less with the observation as the timing is closer to observations in Fig. 14 compared to Fig. 13. The model results predicted relatively higher rainfall amounts than the observed values for maximum rainfall locations in the box (Fig. 14a). However, the total accumulated rainfall predicted by 1.5 km resolution is relatively higher than 330 m resolution, indicating 330 m model under predicted the intensity of the convective activity compared to 1.5 km run. Both 1.5 km and 330 m model results showed an increase in CAPE values from 06 UTC to 12 UTC. During the thunderstorm period, the observations showed decrease in OLR values, which is also reflected in the models though with a higher decrease in OLR indicating more cloudiness simulated by the model.

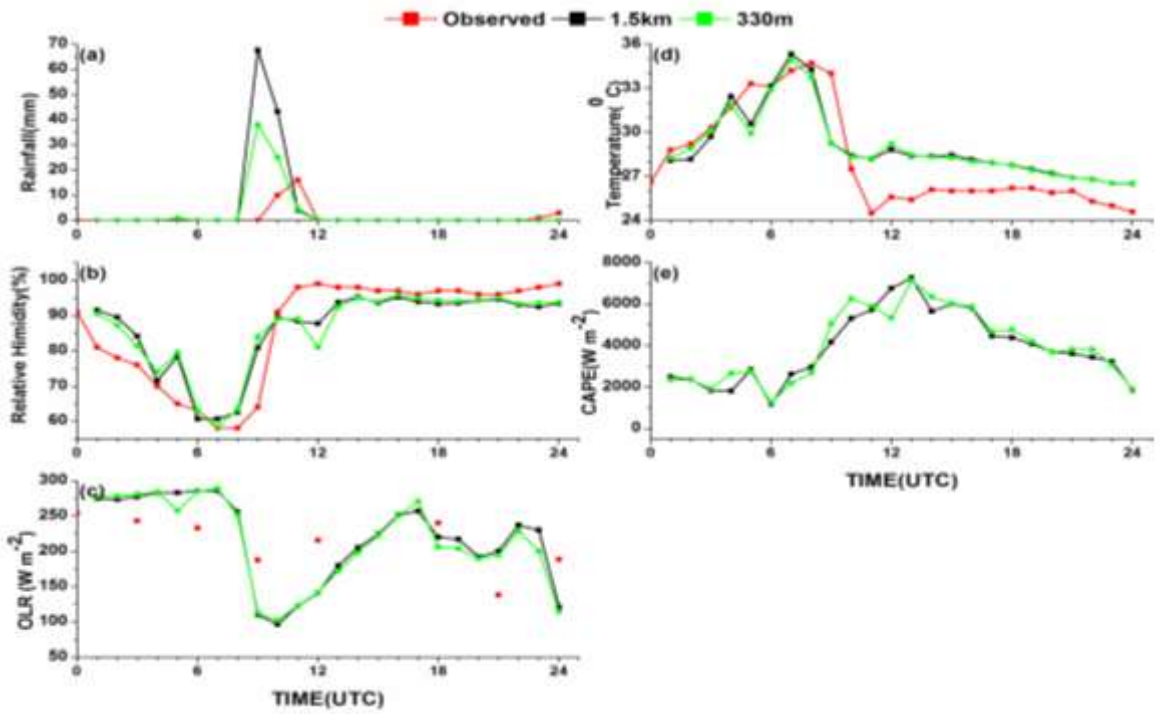

Fig. 14: *Temporal variation of meteorological variables from NCUM regional (1.5 km and 330 m) model, Automated Weather Stations (AWS) and observed (OLR- kalpana-1 VHRR) at 3-hourly maximum rainfall location (lat/lon) over 330 m model domain.*

To compare the intensity of the deep convective activity in 330 m and 1.5 km model domains, the time evolution of the vertical distribution of temperature and vertical velocity at the location of maximum rainfall during the thunderstorm period was analysed (Fig. 15). From the figures, it can be seen that 330 m model failed to predict intense activity and updrafts, compared to 1.5 km model while the latter produced higher surface temperature variations and intense updrafts just before 9 UTC.

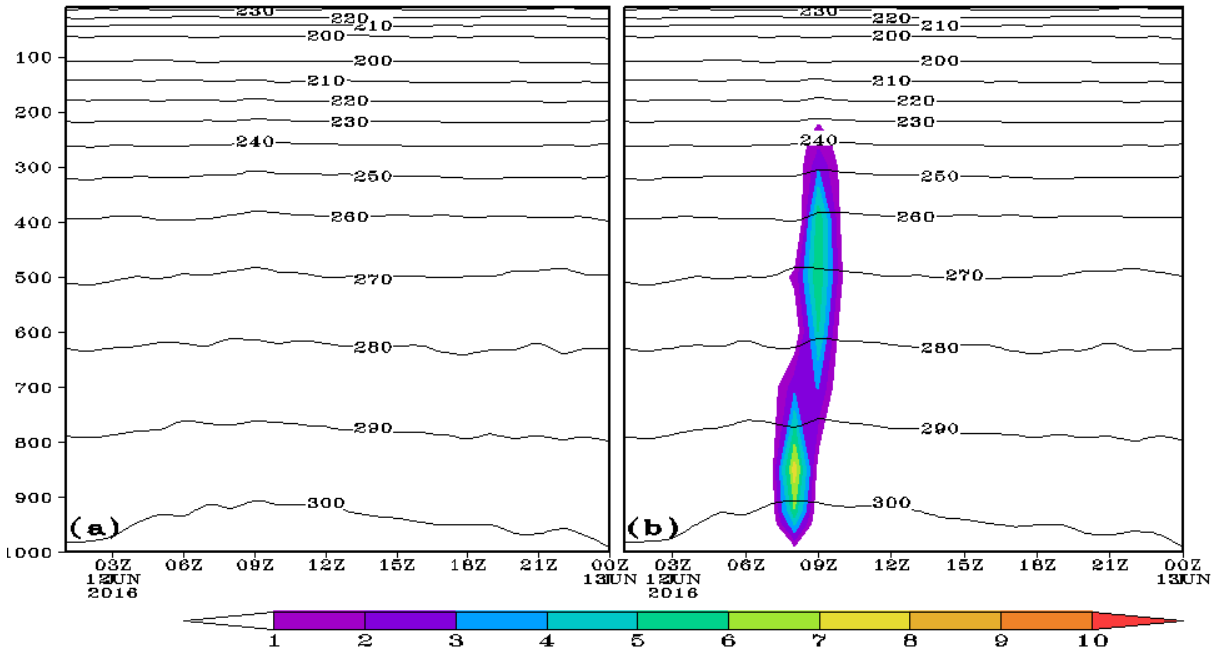

Fig. 15: *Vertical cross-section of the vertical velocity (m/s; shaded) and temperature (K; contour) in (a) 330 m model resolution and (b) 1.5 km resolution.*

5. SENSITIVITY EXPERIMENTS

In the cloud scheme (Smith, 1990), the cloud is permitted to form before the average relative humidity over a grid box reaches 100%. In the global model this value is set to start from the surface as low as 92%, whereas in the convection permitting formulations, it is set as higher as much of the sub grid scale processes are resolved through the explicit moisture processes. In the 330 m model it is set as starting with 97% at the surface level and gradually reducing to 90% at 3.5 km and remains constant above. Sensitivity of the fixed RHcrit profiles, which controls the cloud formation, on the intensity of the convection and the possible formation of thunderstorm, is attempted in this work. The six sensitivity experiments were conducted by changing the RHcrit profiles as described below, starting with the lowest value of 96% as the control and with the corresponding changes proportionally in the vertical.

1) **330mV1:** Lowest level RHcrit value: **96%**

(RHcrit=12*0.960,0.950,0.940,0.930,0.930,0.930,0.920,0.920,0.920,5*0.910,5*0.900,50*0.890**)**

2) **330mV2:** Lowest level RHcrit value: 97%

(RHcrit=12*0.970,0.960,0.950,0.940,0.940,0.940,0.930,0.930,0.930,5*0.920,5*0.910,50*0.900**)**

3) **330mV3:** Lowest level RHcrit value: 99%

(RHcrit=12*0.990,0.980,0.970,0.960,0.960,0.960,0.950,0.950,0.950,5*0.940,5*0.930,50*0.920**)**

4) **330mV4:** Lowest level RHcrit value: 100%

(RHcrit=12*1.000,0.990,0.980,0.970,0.970,0.970,0.960,0.960,0.960,5*0.950,5*0.940,50*0.930**)**

5) **330mV5:** 330mV3 with moisture conservation ON

6) **330mV6:** 330mV1 with moisture conservation ON

The RHcrit values are starting with the lowest level value of 96% (Control), 97%, 99% and 100%, while the moisture conservation is applied to profiles starting from 96% and 99% only to demonstrate the impact of two different marked profiles on the model parameters. Fig. 16 displays the rainfall distribution in the 330 m model domain for each of the experiments and the domain averaged rainfall is provided in Fig. 17. All the simulations show the continuous patterns of the rainfall over the northwest sector and over the valleys of north part of the domain with maximum rainfall over the northwest corner. The slopes over the southern part of the domain features cellular patterns of the rainfall activity though it might be causing more spontaneous thunder developments. Fig. 1 shows the locations of AWS observations with which 3-hourly maximum rainfall (8-11 UTC) over the 330 m model domain for all the experiments were compared with. It can be seen that 330mV3, 330mV5 and 330mV6 are having maximum rainfall location on the slopes over the high terrain region in the southern part of the domain and the locations as well as the terrain heights vary with each experiment. The domain averaged rainfall shows maximum rainfall for 330mV2 with the RHcrit values starting with 97% from the surface level, along with maximum coverage and intensity of the activity from the spatial distribution. With the increase in RHcrit value, the domain mean rainfall generally decreases, though the excessive rainfall areas are increasing. The application of moisture conservation smoothens the excessive rainfall patches. Fig. 18 displays the sensitivity of RHcrit on time variation of the various parameters at the 3 hour window at maximum rainfall locations inside the 330 m domain box for each of the experiments with different RHcrit profiles. Figs. 19 and 20 represent the sensitivity of applying moisture conservation with two contrasting RHcrit profiles. In most of the AWS locations, the model is able to produce some rainfall along with the observed rainfall, though the predicted values are highly variable and do not match with the observations quantitatively

(Fig. 19). We have obtained a mixed kind of results from Fig. 20, few characteristics can be summarised on an overall assessment as given below.

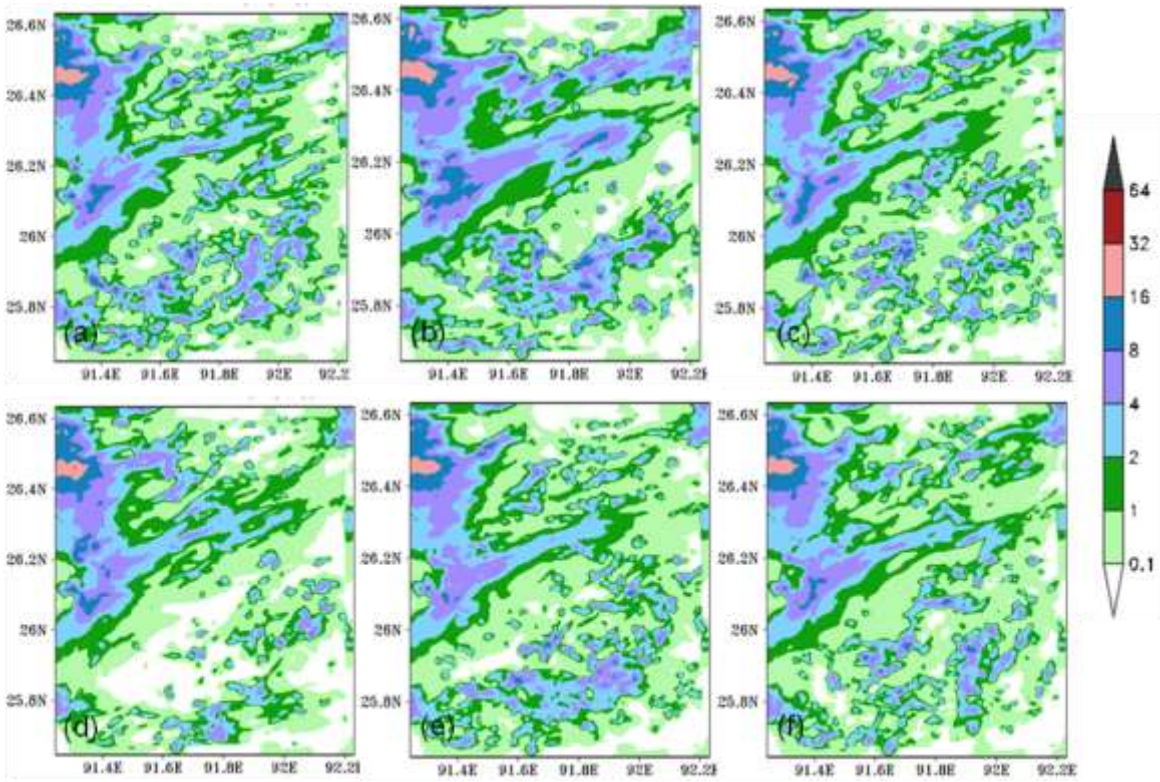

Fig. 16: *NCUM simulated rainfall (mm) for (a) 330mV1, (b) 330mV2 (c) 330mV3, (d) 330mV4 (e) 330mV5 and (f) 330mV6.*

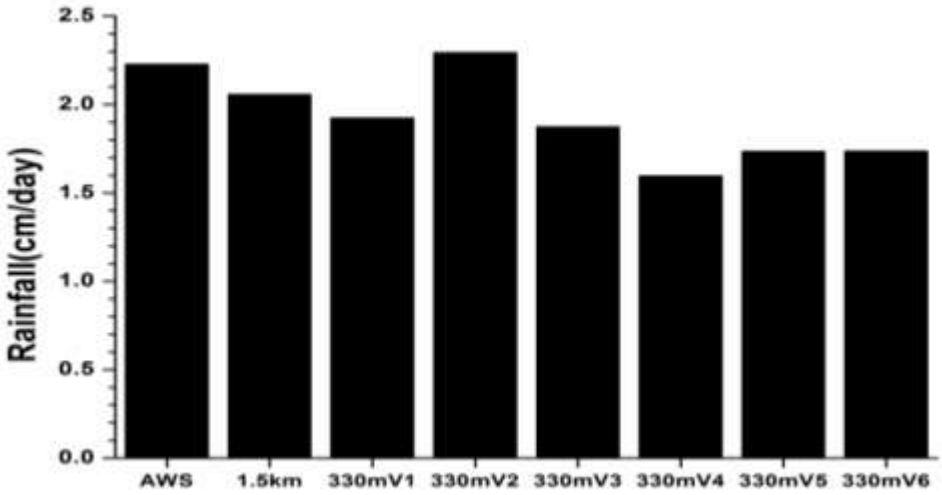

Fig. 17: *Comparison of diurnal variation of area averaged (25.645°N-26.631°N, 91.245°E-92.231°E) rainfall (cm/day).*

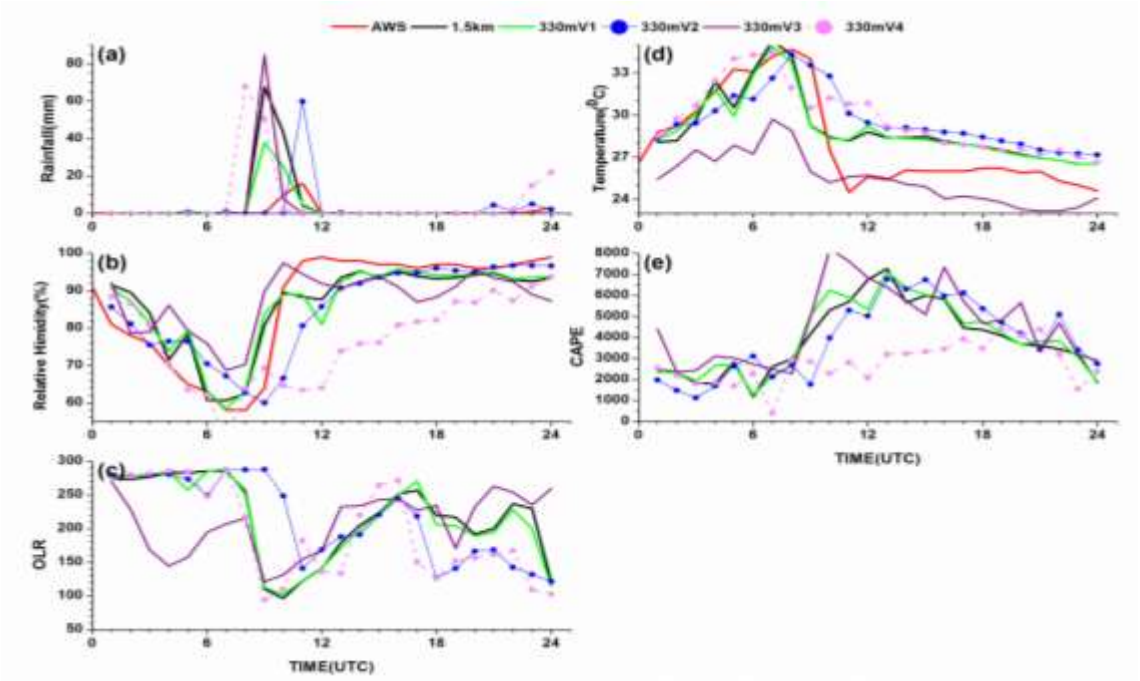

Fig. 18: *(a) Rainfall (mm), (b) 1.5 m relative humidity (%), (c) OLR(W/m^2), (d) 1.5 m temperature (K) and (e) CAPE (J/kg), of 1.5 km and 330 m models with different experimental simulations at the 3-hourly maximum rainfall locations.*

1) As the locations can vary, the rainfall periods and the peak rainfall timings can also vary for the different experiments. Peak rainfall values are higher in the experiments compared to the observations and there is a tendency to predict the peak 1 hour early, except for 330mV2, which is matching with the AWS peak value timing.
2) In general, with the increase in RHcrit, the peak amount of rainfall is also increasing. Also maximum value of the peak rain is observed in 330mV3.
3) None of the experiments could simulate the dip in surface temperature as observed. 330mV3 experiment is showing a lower temperature values comparable with the observations after the event. It also shows relatively lower values of temperature before the event, which is different from the observations and all other experiments.
4) Same is the case for RH in producing comparable higher values as observations after the event, while giving highest values before the event, compared to the observation or other experiments.
5) CAPE and OLR also shows better values for 330mV3 while OLR shows much variability between the experiments.
6) 330mV5 (99% lowest level RHcrit and moisture conservation switched on) shows the maximum rainfall peak, the best match in surface temperature both before and after the event.

The time evolution of vertical profiles of vertical velocity and temperature at the location of maximum rainfall in the 330m model box is shown in Fig. 21 for 330mV1, 330mV3, 330mV5 and 330mV6. Except for 330mV1, all other experiments predicted strong updrafts. 330mV3 shows slight early timing which is resolved in 330mV5. That is, with the lowest RHcrit value of 99% and with moisture conservation switched on, the updrafts are well simulated by the model at 9 UTC. Also there is a shallow upward motion observed above the surface layers just before 9 UTC.

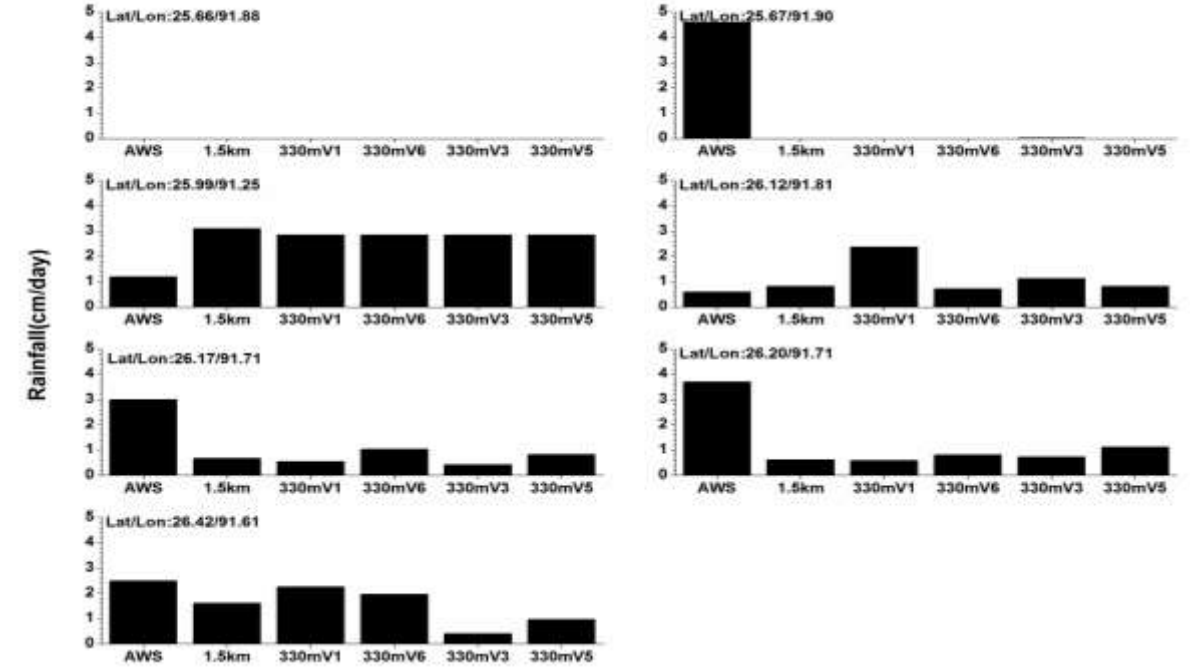

Fig. 19: *The model rainfall (mm) at the AWS observation locations for 330mV1, 330mV3, 330mV5 and 330mV6.*

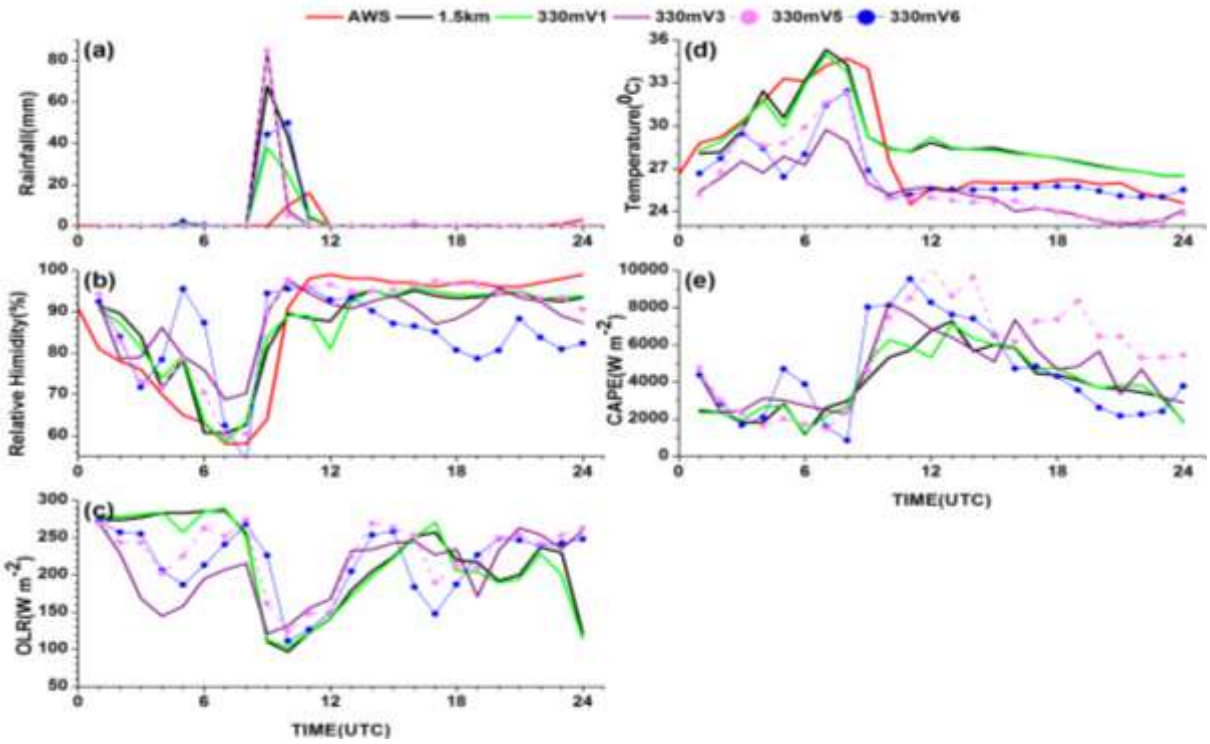

Fig. 20: *Same as Fig. 18 but with and without moisture conservation*

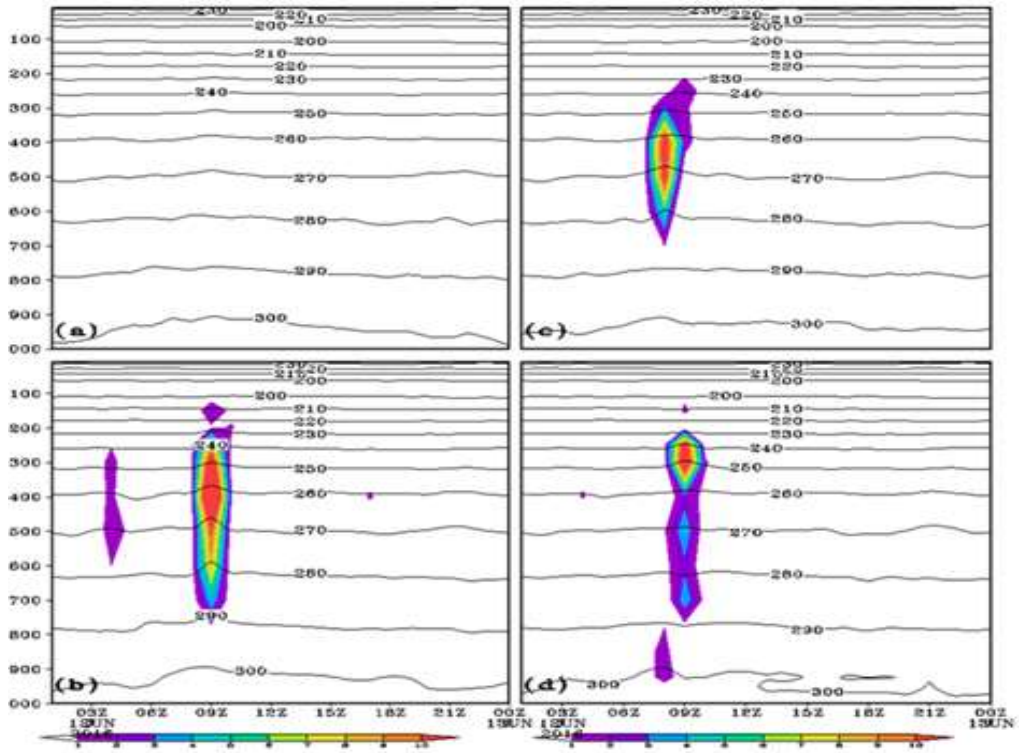

Fig. 21: *Vertical cross-section of the vertical velocity (m/s; shaded) and temperature (K; contour) in 330 m model with different experiments (a) 330mV1, (b) 330mV6, (c) 330mV3 and (d) 330mV5.*

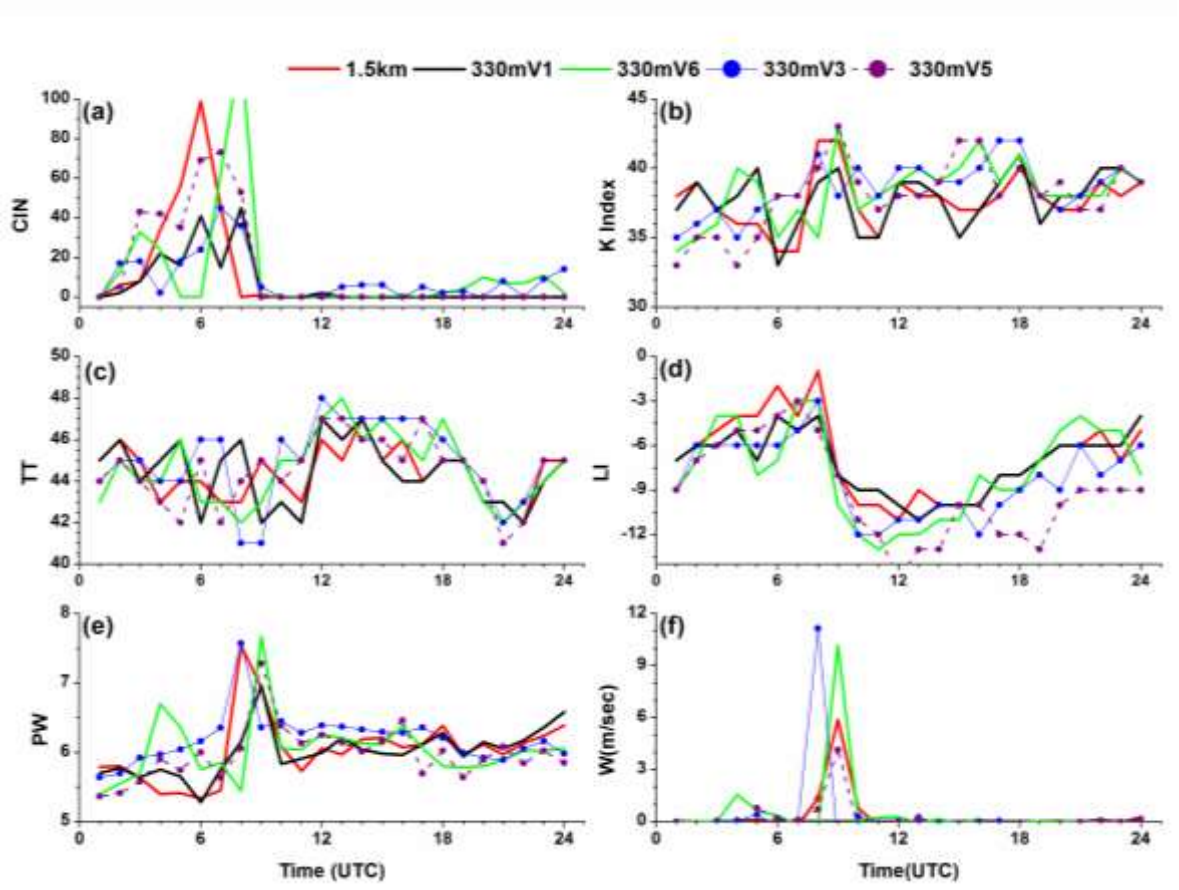

Fig. 22: *(a) Convective Inhibition (CIN; J/kg), (b) K index (KI), (c) Total totals index (TT), (d) Lifted index (LI), (e) Precipitable Water (PW; cm) and (f) Vertical Velocity (W; m/s) at 500 hPa.*

Many stability indices have been developed as preconditions for the likely thunderstorm formation based on the atmospheric stability, relative humidity, wind shear and a source of trigger (Haklander and Van Delden, 2003). As the thermodynamic indices play a significant role in understanding and prediction of the thunderstorm, we computed some of those parameters (like Convective Inhibition - CIN, Totals Totals - TT, Precipitable Water - PW, K Index -KI, Lifted index - LI, and vertical velocity at 500 hPa - W) from the model (Fig. 22).

Convective available potential energy (CAPE) and convective inhibition (CIN) are the two primary thermodynamic parameters for assessing the occurrence of deep moist convection in the atmosphere. The CAPE represents a measure of energy available to a rising cloud parcel, and in conjunction with dynamical parameters such as the wind shear, has been used to determine the nature of the resulting convective systems. The CIN is a measure of the energy required by a rising air parcel to reach its level of free convection (LFC): this is

'activation energy' for the system. KI is used for determining what the probability and spatial coverage of ordinary thunderstorms would be based on temperature and dew point temperature. If storms form, LI is an index that indicates the severity of the storms. TT gives an indication for the probability of seeing severe thunderstorm activity.

Several researchers used the threshold values (**TT >44, LI < -6, K>35, CAPE>1500**) of these thermo-dynamical indices to be the prerequisites for the thunderstorm occurrence (Vujovic et al., 2015; Wilks, 2006; Haklander and Van Delden, 2003; Kunz, 2007; Tyagi, 2011). The thunderstorm thermo-dynamical indices/parameters are simulated with 1.5 km and 330 m model resolutions for the set of four experiments with lowest level RHcrit values of 96% and 99% and without and with moisture conservation and are depicted in Fig 22. The maximum CIN values for 1.5 km, 330mV5 and 330mV6 are observed at 06 UTC, 07 UTC, and 08 UTC respectively. Around 09 UTC, a decrease in CIN values from their peaks to near zero values is observed just before the occurrence of thunderstorm. However, at the time of thunderstorm an increase in CAPE values was observed (Fig. 20e). In all the model results, the K index values are relatively high during the thunderstorm periods when compared to others timings. During the thunderstorm period, the K index values of above 40 are observed by 1.5 km resolution, 330mV3, 330mV5 and 330mV6.

During the thunderstorm period, the experiments 330mV3, 330mV5, 330mV6 the TT values show an increasing trend after the occurrence of thunderstorm. But during the thunderstorm period there is an oscillation of TT values for all the experiments and 330mV3 achieves the lowest values. A threshold value of -6 in LI is a good indicator of thunderstorm occurrence. Both 1.5 km resolution and all the experiments of 330 m resolution (330mV1, 330mV3, 330mV5, and 330mV6) showed a sudden decrease in LI (below -6) at the time of thunderstorm. The updrafts in the mature stage of thunderstorm are relatively higher when compare to the initial and dissipating stages of the thunderstorm. This phenomenon was clearly reproduced by both 1.5 km resolution and all the experiments of 330 m resolution (330mV1, 330mV3, 330mV5, and 330mV6). However, when compared to other experiments (1.5 km resolution, 330mV1, and 330mV5), 330mV3 and 330mV6 experiments predicted relatively higher updrafts. Even though the 1.5 km and different experiments of 330 m resolution predicted the thunderstorm parameters reasonably well, the experiments 330mV5, 330mV6 had fairly good accuracy.

As shown earlier the vertical velocity values (W) are the most critical parameter defining the possibility of any thunderstorm event which is almost absent in the control run (330mV1). All the experimental runs showed W values of various intensities and 330mV3

displayed maximum vertical velocity simulated by the 330 m model. However, the timing is showing a phase shift as 330mV3 predicts the event before 9 UTC. 1.5 km resolution, 330mV5 and 330mV6 all are consistent in predicting the peak timings. The 330mV6 predicts the maximum peak updrafts, which indicates that the moisture conservation is having a significant impact on the simulated updrafts and rainfall. However, 330mV6 seems to be over-predicting the event while 330mV5 appears to be the overall best in all aspects. Hence considering all the parameters, combining the RHcrit values starting with 99% together with the moisture conservation is the best suited science configuration for thunderstorm simulation in 330m resolution models.

6. SUMMARY AND CONCLUSIONS

The accurate predictions of severe thunderstorms have paramount importance on the socio-economy of India. The case study of a thunderstorm event occurred on 12 June 2016 at Guwahati located over the north east region of India using NCUM-R at 1.5 km and 330 m resolutions is described. In the current work, an analysis of the skill of NCUM model at various resolutions ranging from global to 330 m, was undertaken to understand its role as a potential tool in the practical application of the thunderstorm prediction. It was established that global model resolution with 17 km grid spacing does not show any signatures of a thunderstorm at Guwahati though the domain averaged features are showing synoptically favourable conditions over a larger region. The high resolution runs were validated for their large scale conditions and the environmental feedbacks during the period of the thunderstorm. Spatial and temporal validation and comparison of thunderstorm parameters between the model and the observations were carried out. As it is difficult to predict accurately the location specific rainfall with very high resolution models, a small box that of the 330 m model was considered to check whether the model is able to predict favourable conditions for a thunderstorm development anywhere in this small domain. The comparison of the parameters was carried out at maximum rainfall location in each simulation, whereas the locations can vary in each experiment with its varying surface terrain characteristics. It was found that 1.5 km resolution model was able to simulate the thunderstorm signatures in a better way in terms of intensity compared to 330 m runs. During thunderstorm period, 1.5 km model results showed a vertical profile of strong updraft, strong potential vorticity, strong convergence and divergence, high specific humidity and a sharp variation in temperature. But, 330 m model is unable to predict the strong updraft and potential vorticity at the time of thunderstorm anywhere in the domain.

Hence, for improving the 330 m model performance, we run with various RHcrit values with and without moisture conservations. RHcrit influence the cloud formation at a grid where the cloud can form much before the mean relative humidity in a grid box reaches 100%, thus can alter the thermodynamic profile in the vertical. With the increase in RH critical values, the model has in general increased rainfall and vertical velocity. By changing the RHcrit values (with and without moisture conservation), the 330 m model results showed an improvement in the updraft and temporal variation of surface temperature, surface humidity and rainfall during the period of thunderstorm. Similarly, during the thunderstorm period, both 1.5 km and 330 m model results predicted the favourable values of thermo-dynamical parameters. When compared to all the experiments the RHcrit values starting at lower level at 99% with moisture conservation (330mV5) is found to be the best combination of model physics in the overall simulation of the extreme convective activity.

REFERENCES

Best MJ, Pryor M, Clark DB, Rooney GG, Essery RLH, Ménard CB, Edwards JM, Hendry MA, Porson A, Gedney N, Mercado LM, Sitch S, Blyth E, Boucher O, Cox PM, Grimmond CSB, Harding RJ. 2011: The Joint UK Land Environment Simulator (JULES), model description. Part 1: energy and water fluxes. *Geoscience Model Development 4*, 677–699. https://doi.org/10.5194/gmd-4-677-2011.

Edwards JM, Slingo A. 1996: Studies with a flexible new radiation code. I: choosing a configuration for a large-scale model. *Quart. J. Roy. Meteorol. Soc. 122*, 689–719.

Gregory J. 1999: Representation of the radiative effects of convective anvils. *Hadley Centre Tech. Note 7. Met Office: Exeter, UK*.

Haklander, A. J., and A. Van Delden 2003: Thunderstorm predictors and their forecast skill for the Netherlands. *Atmos. Res., 67–68*, 273–299.

Jayakumar A, Sethunadh J, Rakhi R, Arulalan T, Mohandas S, Iyengar G R, Rajagopal E. N., 2017: Behavior of predicted convective clouds and precipitation in the high-resolution Unified Model over the Indian summer monsoon region. *Earth and Space Science 4:* 303–313. https://doi.org/10.1002/2016EA000242.

Kunz, M., 2007: The skill of convective parameters and indices to predict isolated and severe thunderstorms. *Nat. Hazard Earth Sys.*, 7, 327-342.

Lilly, D. K., 1990: Numerical prediction of thunderstorms—Has its time come? *Quart. J. Roy. Meteorol. Soc., 116*, 779–798.

Rakhi R., Jayakumar A., Sreevathsa M.N.R., Rajagopal E.N., 2016: Implementation and up-gradation of NCUM in Bhaskara HPC. *NMRF/TR/03/2016*,

https://doi.org/10.13140/RG.2.1.4624.7923.

Smith RNB. 1990: A scheme for predicting layer clouds and their water content in a general circulation model. *Quart. J. Roy. Meteorol. Soc., 116,* 435–460. https://doi.org/10.1002/qj.49711649210.

Tyagi, B., Krishna, V.N., Satyanarayana, A.N.V., 2011: Study of thermodynamic indices in forecasting pre-monsoon thunderstorms over Kolkata during STORM pilot phase 2006–2008. *Nat. Hazards, 56*, 681-698.

Vujovi´c, D., Paskota, M., Todorovi´c, N., Vuˇckovi´c, V., 2015: Evaluation of the stability indices for the thunderstorm forecasting in the region of Belgrade, Serbia, *Atmospheric Research*, doi: 10.1016/j.atmosres.2015.04.005

Wilks, D.S., 2006: Statistical methods in the atmospheric sciences. *Academic Press, London,* pp 627.

Wilson, D. R., and S. P. Ballard, 1999: A microphysically based precipitation scheme for the U.K. Meteorological Office Unified Model, *Quart. J. Roy. Meteorol. Soc., 125*, 1607–1636, doi:10.1002/qj.49712555707

Wood, N. J., et al., 2014: An inherently mass-conserving semi-implicit semi-Lagrangian discretization of the deep-atmosphere global non-hydrostatic equations, *Quart. J. Roy. Meteorol. Soc., 140*, 1505–1520.